Desalination and Water Treatment
www.deswater.com
doi: 10.5004/dwt.2023.29162

284 (2023) 61–71
February

The applications and modification of MXene-based absorbents: a review

Yucheng Liu[a,b,*], Jiahao Mei[a], Mingyan Chen[a,b], Lili Ma[a,b], Lingli Li[a,b], Bing Yang[a,b], Wenwen Tu[a]

[a]*College of Chemistry and Chemical Engineering, Southwest Petroleum University, Chengdu, Sichuan 610500, P.R. of China, emails: 1054948240@qq.com (J. Mei), tt20190828@sina.com (W. Tu)*
[b]*Research Institute of Industrial Hazardous Waste Disposal and Resource Utilization, Southwest Petroleum University, Chengdu, Sichuan 610500, P.R. of China, Tel. +86 13551308326; email: rehuo2013@sina.cn (Y. Liu), cmyswpi@126.com (M. Chen), hjxymall@163.com (L. Ma), 201699010021@swpu.edu.cn (B. Yang), 704817808@qq.com (L. Li)*

Received 24 July 2022; Accepted 27 November 2022

ABSTRACT

Water treatment demands have intensified increased due to aggravated environmental pollution. Finding materials to remove toxic contaminants, which include heavy metal ions, organic dyes and radionuclides, have become highly urgent. Adsorption, as one of the widely used water purification technology, has attracted much attention because of its low cost and high efficiency. Traditional adsorbent's applications are limited by their poor selectivity, high recycling cost, and small specific surface area. MXene, an emerging two-dimensional layered material, has attracted much attention owing to its excellent hydrophilicity and adjustable surface properties. Particularly, in the domain of adsorption. A large number of MXene-based adsorbents have shown great promising in numerous researches. Based on this, in order to understand the adsorptive behavior of MXene-based materials, a detailed and comprehensive review is necessary. The purification progress via MXene-based adsorbents is easy to be affected by not only the operating condition of application but also the structure of materials, such as interlayer space and surface group composition. Therefore, this review summarizes recent advances in water treatment via MXene-based adsorbents. The synthesis of MXene used in adsorption is presented. The effect of the structure of MXene on the adsorption of various contaminants by comparing the previous data of the kinetics, isotherms and uptake capacity is discussed. Finally, this article also covers those strategies that can elevate adsorption capacity by changing the structure of MXene.

Keywords: MXene; Synthesis; Adsorption; Structure

1. Introduction

The requirement for high-quality water has increased as a results of population development and industrialization [1]. So far, more than 700 different contaminants have been discovered in natural water [2]. Among them, heavy metals, organic dyes, and radioactive elements have become widely researched objects due to their non-biodegradability, gene mutation, and carcinogenicity [3,4]. Numerous removal methods for the three types of pollutants mentioned above have been developed, including chemical precipitation [5], advanced oxidation [6], ion-exchange [7], membrane separation [8], and adsorption. However, the complex composition of wastewater poses a severe application limitation for above technologies. Adsorption technology has attracted great attention because of its low cost and high efficiency. A large number of natural materials has been considered absorbents with certain adsorption capacity, such as kaolinite [9], activated carbon, and bentonite clay [10]. While, the defects such as low selectivity, high recycling cost, and the large volume

* Corresponding author.

of traditional natural adsorption materials hindered their practical applications. Recently, two-dimensional materials have been considered one of the most promising adsorbents [11–13]. With a large specific surface area, these two-dimensional materials have exhibited excellent removal capacity for pollutants [12]. MXene, an emerging two-dimensional material, has attracted much attention in water treatment due to its abundant surface groups, high hydrophilicity and structural stability [4].

MXene is produced from the layered ternary MAX phase. MAX phase is a general term for various different metal nitrides or carbides, which conform to the formula of $M_{n+1}AX_n$. Where "M" represents the early transition metals, the "A" is the elements of group IIIA or IVA, "X" is carbon or nitrogen and the "*n*" generally takes from one to four [14]. Owing to the differences in relative strengths of the M-A bonds and M-X bonds, MXene can be obtained by removing the "A" layer atoms from the MAX phase via hydrofluoric acid (HF) etching [15,16]. The general formula of MXene is $M_{n+1}X_nT_x$ (n = 1, 2, 3). Here, the "T" represents the surface terminal group such as −O, −F, –Cl and −OH. The symbol "x" is the number of surface groups.

In recent years, MXene-based materials have been used for water purification as an adsorbent [17–19]. These studies have confirmed that MXene-based adsorbents can remove various environmental contaminants owing to their abundance of active sites, hydrophilic nature and high surface area. With the development of various MXene-based adsorbents and modification strategies, it is extremely important to comprehensively understand the relationship between the structure and adsorption performance of MXene to improve its application performance.

This review focuses on the scientific advances in the water purification of MXene as the adsorption material over the past decade. Although some review articles on MXene in the field of water treatment have been published, they either focused on the comprehensive application or targeted other particular domains. For example, one study reviewed the synthesis, characteristics, and comprehensive environmental applications of MXene [20], while another looked at MXene-based water treatment membranes [21]. However, few review papers focused on the effects of the structure of MXene on adsorption properties. Furthermore, since numerous MXene adsorption materials have been developed and applied to water purification; therefore, in order to scientifically design MXene-based adsorbent, it is necessary to pay more attention to the influence of the structure of MXene on adsorption performance. This present review briefly introduces the preparation methods of MXene materials used in the adsorption domain and analyzes the relationship between the structure of MXene, especially the topography and group composition, and adsorption performance by comparing the thermodynamic, kinetic, and adsorption data from the previous reports. Finally, we summarize those strategies that can elevate sorption capacity by changing the structure of MXene.

2. Synthesis and surface chemical properties

Until now, more than thirty kinds of MXenes have been obtained by selective removal of A-layers atoms from nitride, carbide, or carbo-nitride. According to different preparation methods and MAX precursor phases, the atomic structures of these MXenes can be classified into three types: M_2XT_x, $M_3X_2T_x$, and $M_4X_3T_x$ [22]. Generally, most of the MXenes used for adsorption are $M_3X_2T_x$. There are two main strategies for the synthesis of MXene, summarized as top-down and bottom-up mechanisms. The former mechanism corresponds to the exfoliation of MAX precursor into single-layered MXene sheets, and the latter concentrates on the growth of MXene from atoms or molecules. Most of the current preparation routes belong to the former strategy, which includes HF etching, *in-situ* HF etching, alkali etching, etc. These preparation methods endow MXene with unique structure and surface properties reflected in exterior groups and interlayer spacing. Here, only the common preparation methods of MXene used in adsorption are introduced.

2.1. HF etching

Most parts of MXenes-based adsorbents reported to date are generally synthesized by etching in HF, and this method was first proposed in 2011 [15]. The etching process involves the destruction of M-A bonds by strong acids and the formation of surface group structures [20,22,23]. The following are the reaction equations:

$$Ti_3AlC_2 + 3HF = AlF_3 + \frac{3}{2}H_2 + Ti_3C_2 \quad (1)$$

$$Ti_3C_2 + 2H_2O = Ti_3C_2(OH)_2 + H_2 \quad (2)$$

$$Ti_3C_2 + 2HF = Ti_3C_2F_2 + H_2 \quad (3)$$

As can be seen from the above reaction equations, –OH, –F groups are formed on the MXene surface by this method, which imparts MXene good hydrophilicity and dispersibility to be a great adsorbent to treat water. Due to van der Waals forces, the production in this way has a restack trend to form an accordion-like structure (Fig. 1) [24]. This unique structure makes layer spacing one of the main factors affecting MXene adsorption. Different process conditions may lead to the distinction of interlayer spacing [16]. It will be discussed in Section 2.4 – Synthesis conditions and structure characteristics.

Simple operation and considerable laboratory yield are the advantages of this method. But the HF etching process involves the usage and post-use treatment of HF solution, which is extremely dangerous for operators. Hence, the development of more safety and environmentally compatible methods for MXene synthesis is warranted.

2.2. In-situ HF etching

To avoid the hazardous and toxic impact of HF, an alternate way of preparing MXene has developed. Less hazardous acids (such as hydrochloric acid or sulfuric acid) can be used to form hydrofluoric acid with fluoride salts, such as KF, NaF, NH_4F and FeF_3 [26,27]. The reaction

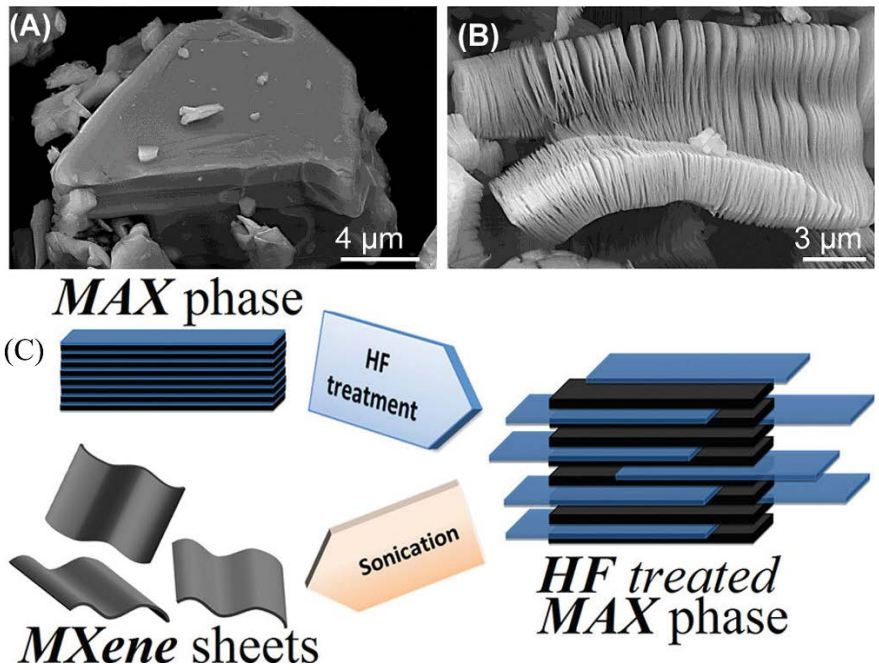

Fig. 1. Morphological structure of (A) Ti_3AlC_2 phase before HF treatment, (B) accordion-like structure of Ti_3C_2 after HF etching and (C) schematic of the exfoliation process from MAX phases to multilayer MXene. Reproduced with permission Naguib et al. [25]. Copyright 2012, American Chemical Society.

mechanism is the same as HF etching. Theoretically, fluoride salts formed by the elements of the first groups can be used to prepare MXene [20]. Compared to HF etching, the resulting product by this way has a larger layer spacing owing to the cationic intercalation effect. It can be characterized by the *c* lattice parameter. For example, the *c* lattice parameter of $Ti_3C_2T_x$ etched by hydrofluoric acid is only 1.98 nm, while that of the same $Ti_3C_2T_x$ etched by fluoride salts is 2.47 nm [28].

In addition, MXene produced in this way possesses few defects and a larger lateral size [28–30]. Based on the above, it is one of the most commonly used methods for the preparation of MXene adsorbents.

2.3. Intercalation and delamination

Intercalation and delamination are two major processes for getting single-layered MXene. Both HF etching and *in-situ* HF etching produce multilayered MXene samples, which results in a limited specific surface area of MXene, and some adsorption sites are unavailable. Intercalation is conducted after etching to expand the space between the layers of accordion-like MXene, and delamination is conducted after intercalation to produce single-layered MXene to get a larger specific surface area and release more active sites. The common intercalants include dimethyl sulfoxide, tetraalkylammonium compounds, alkaline solutions and water molecules [30]. Delamination can be achieved by three methods: centrifugation alone, hand-shaking and sonication. Hand-shaking separates multilayered $Ti_3C_2T_x$ powder, produced by (7.5 M LiF/9 M HCl), into single and obviously large flakes [31]. It resulted in a few defective single flakes and a higher concentration of MXene [22]. Sonicating results in smaller flakes with more defects and may also yield higher concentrations.

2.4. Synthesis conditions and structure characteristics

So far, all MXenes produced by the methods described above always have surface terminations such as fluorine, oxygen, or hydroxyl, which impart hydrophilicity to their surfaces and make them suitable for adsorption [32]. Different preparation methods and process conditions affect the product structure of MXene. It is mainly reflected in surface groups and interlayer spacing.

The MXene made by HF have more –F groups and less oxygenated groups than that synthesized by the *in-situ* HF method (Fig. 2) [33]. The process conditions also have an influence on the proportion of different surface groups. With the concentration of HF increased from 5 to 30 wt.%, the proportion of –F terminations increased by 11.66% (from15.85% to 27.51%), and the oxygen-containing terminations decreased by 7.77% (from 16.59% to 8.82%) [14]. The –F group has a better affinity for cationic dyes than –O, while Oxygenated groups, such as –OH and –O, have better for heavy metal ions and radionuclides [34–36]. Therefore, the appropriate preparation method can be selected according to the contaminant. Interestingly, the heating process promotes the change of surface groups from –F to –O, and even makes part of the MXene surface bare [37]. It allows further functionalization according to the application demand of adsorption.

Interlayer spacing is an important structure parameter for adsorption; narrower interlayer spacing prevents pollutants from interlayer space, thereby limiting the number of react sites and decreasing the adsorption capacity [38].

The interlayer spacing was affected by etching conditions and intercalation of organic solvents, cations and water molecules in the preparation process [22,30]. At a unified reacting time (24 h) and temperature, when the HF concentration increased from 10 to 25 wt.%, the interlayer spacing was enlarged; but with the HF concentration increased from 25 to 50 wt.%, the interlayer spacing was shrunken. It is attributed to the formation of ternary fluorides and long etching time [14,22,39]. Regarding the effect of temperature, there is a positive correlation between reaction temperature and layer spacing [14,40]. Regarding the influence of intercalants, after treatment with 5% NaOH solution, the surface areas of Alk-$Ti_3C_2T_x$ (76.42 m^2/g) are much bigger than $Ti_3C_2T_x$ (9.78 m^2/g), which can be attributed to the enlargement of the interlayer spacing by intercalation of Na^+ [41]. These intercalants expand the interlayer spacing by weakening the van der Waals forces through ion-exchange and osmotic swelling [24].

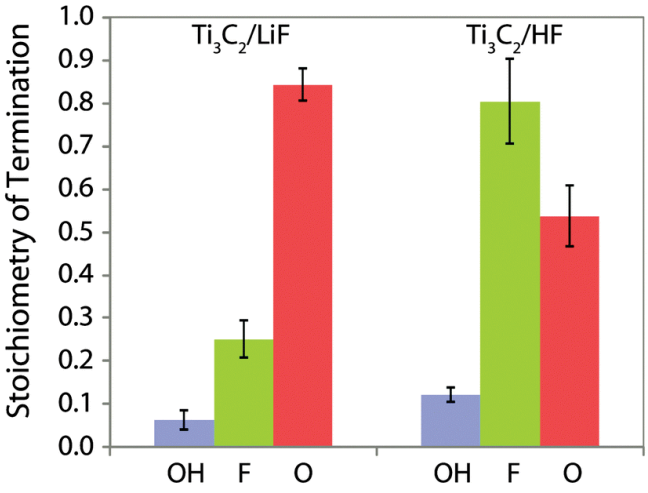

Fig. 2. Composition of the $Ti_3C_2T_x$ surface functional groups produced by HF etching of Ti_3AlC_2 and *in-situ* HF etching of Ti_3AlC_2. Reproduced with permission Hope et al. [33]. Copyright 2016, Royal Society of Chemistry.

3. Adsorption application

3.1. Heavy metal

Removing heavy metal contaminants has attracted much attention because of their high toxicity to organisms. Pb(II), Cr(IV), Hg(II), Cd(II), and Cu(II) are standard pollutant components in the wastewater. Due to the complex composition of polluted wastewater and the refractory biodegradability of heavy metals, adsorption is considered to be the most effective way to remove heavy metal ions. Heavy metal ions can be adsorbed by MXene through interactions such as electrostatic attraction [39], ion-exchange [18], and chelation [42]. So far, numerous studies on the removal of heavy metal ions by MXene-based adsorbents have been carried out, as shown in Table 1. In this section, the effect of operating conditions and structure of MXene-based absorbent on adsorption efficiency were discussed.

Numerous researches have shown that adsorption performance is associated with oxygen exchange sites, such as –OH, –O–. According to First-Principles Calculations, the adsorption efficiency of heavy metal ions for MXene is restrained by –F groups [36]. The surface group of MXene can be altered by functionalization. For instance, Peng et al. [44] reported that the MXene treated with alkalization has a better adsorption effect than pristine. After alkalization, the X-ray diffraction (XRD) spectrum revealed a decrease in the F peak as well as the presence of a Na peak. It indicates that the alkalization process involves the conversion of –F to –OH and the intercalation of Na^+. With similar group modification, the Alk-Ti_3C_2 exhibits improved Ba^{2+} treatment performance, with maximum Ba^{2+} adsorption reaching

Table 1
Comparison of MXene-based adsorbent for heavy metal removal

Material	Pollutant	pH	Temperature (°C)	Pollutant concentration (mg/L)	Materials dose (mg/L)	Maximum uptake (mg/g)	References
Ti_2CT_X-EHL	Pb(II)	1–6	30	200	1,600	233	[18]
$Ti_3C_2T_X$-NH_2	Pb(II)	6.3	5	25	100	385	[42]
$Ti_3C_2T_x$-KH570	Pb(II)	1–6	30	500	1,280	147	[43]
Alk-$Ti_3C_2T_x$	Pb(II)	5.8–6.2	0	100	400	140	[44]
Ti_3C_2@IMIZ	Cr(VI)	2	25	30	200	184	[45]
$Ti_3C_2T_x$	Cr(VI)	2	25	50	200	170	[46]
Alk-Ti_2C	Cd(II)	2–9	25	19–561	330	326	[47]
Magnetic $Ti_3C_2T_x$	Hg(II)	2–9	25	10	25	1,128	[48]
$Ti_3C_2T_x$/sodium alginate balls	Hg(II)	6	25	25	1,667	933	[49]
$Ti_3C_2T_x$	Hg(II)	1–6	30	100	500	1,057	[50]
$Ti_3C_2T_X$-PDOPA	Cu(II)	1–11	25	10	200	47	[51]
$Ti_3C_2T_x$	Cu(II)	1–6	25	25	500	79	[52]
Alk-MXene/LDH	Ni^{2+}	1–14	25	100	100	223	[53]
$Ti_3C_2T_x$	Ba^{2+}	3–9	25	1–50	250–500	9	[54]

46.46 mg/g, nearly three times that of pristine $Ti_3C_2T_x$ [41]. As predicted by the density-functional theory (DFT) result, the negative formation energies for the adsorption of Pb^{2+}, Cd^{2+}, Cu^{2+}, Pd^{2+}, and Zn^{2+}, indicate that Alk-MXene is an ideal material for removing heavy metals [36]. This great improvement was attributed to the abundant activated Ti–OH sites, they trap for heavy metal ions by electrostatic attraction and ion-exchange after deprotonation.

The hydrated radius of most metal ions is larger than the layer *d*-spacing for MXene, which prevents metal ions from entering the layer of MXene, which may reduce the adsorption capacity [55]. Hence, for multilayer MXene, interlayer spacing is an essential factor in adsorption. Alkalization further enlarges the interlayer spacing by intercalating cations for more adsorption sites and faster adsorption [44,56]. For Pb(II), Alk-Ti_3C_2 showed an adsorption capacity of up to 140 mg/g, which can be considered high compared to other two-dimensional adsorbents (Pb(II) adsorption by GO–COOH, 96.21 mg/g) [44,57]. Moreover, Alk-Ti_3C_2 attained equilibrium in almost 120s, 15 times faster than pristine $Ti_3C_2T_x$, owing to its enlarged interlayer spacing, which may result in rapid reaction with Pb(II) [58]. Likewise, the presence of hydrophilic groups and weak bonding forces can bind more water molecules, increasing the c-lattice parameters with multilayers of water inserted between MXene nanosheets, allowing more metal ions to combine with MXene [55].

Temperature influences the adsorption efficiency by affecting the diffusion of the metal ions from water to the adsorbent [59]. The effect of temperature on adsorption was investigated by thermodynamic test and adsorption isothermal model. Major reports showed a similar tendency: the negative value of $\Delta G°$, the positive value of $\Delta H°$, and the positive value of $\Delta S°$, which represent the spontaneous, endothermic, and increased disorder of adsorption [45,48,52,60]. $\Delta H°$ also reflects the energy information of the force involved in the adsorption process. The energy of 4–10 kJ/mol for van der Waals forces, 5 kJ/mol for hydrophobic bond forces, 2–40 kJ/mol for hydrogen bond forces, and 40 kJ/mol for coordination exchange [61]. For instance, $\Delta H°$ of Ni(II) adsorption on Alk-MXene/LDH is 8.96 kJ/mol; the mechanism can be illustrated by weak interaction such as van der Waals force [53]. $\Delta H°$ of Hg(II) adsorption on MXene/Fe_2O_3 is 47.56 kJ/mol, reflecting the ion-exchange in this process [48]. The negative value of $\Delta S°$ also indicates that no substantial variation changed in the internal structure of the adsorbent during the sorption process [61].

In summary, the adsorption performance of MXene-based materials is attributed to the interaction between the surface group and adsorbate. The modification method of increasing the layer spacing and the active site can theoretically improve the adsorption performance of MXene.

3.2. Dyes

Dyes are typical synthetic organic compounds with complex structures and are not treated by only single chemical progress. Adsorption is the optimal choice for the removal of dyes. Generally, MXene-based adsorbents are negatively charged, which are inclined to attract the positively charged dyes to achieve wastewater purification.

The adsorption mechanisms, as numerous studies mentioned, are electrostatic interaction [34], ion-exchange [62], and hydrogen bonding [63]. The detailed mechanism is shown in Fig. 3a–c. The remove behavior of dyes compounds has been explored by previous studies. These processes generally effected by many factors such as temperature, pH, and competing ions. Here, the relationship between the structure of MXene and adsorption performance is discussed. The removal for organic contaminants by MXene-based absorbents as shown in Table 2.

Mashtalir et al. [71] reported the adsorption performance of multilayer MXene for cationic methylene blue (MB) and anionic Acid blue (AB80). The study showed that under dark conditions, the concentration of MB decreased rapidly within 8 h, while the concentration of AB80 remained unchanged after 20 h. It can be attributed to the electrostatic interaction between positive-charged MB and negative-charged MXene. Structure changes were also observed in the adsorption process. XRD spectrum showed that the *c*-lattice parameter of MXene increased by 2.0 Å due to partial wedging-in of MB molecules at the edge of MXene [71]. The surface group structure is also regarded as an essential factor for dye removal. Recent

Table 2
Comparison of dye adsorption by various MXene-based materials

Material	Pollutant	pH	Temperature (°C)	Pollutant concentration (mg/L)	Materials dose (mg/L)	Maximum uptake (mg/g)	References
Few-layer Ti_2CT_x	MB	2–10	35	100–1,500	500	2,461	[64]
$Ti_3C_2T_x$/sodium alginate	MB	7	25	100	50	92	[65]
V_2CT_x	MB	5–11	25	20	150	111	[66]
$Ti_3C_2T_x$	MB	7	20	10	100	140	[62]
Sulfonic acid $Ti_3C_2T_x$	MB	7	25	50	10	111	[67]
Alk-$Ti_3C_2T_x$	MB	7–7.2	25	50	500	189	[68]
Polypyrrole/$Ti_3C_2T_x$	MB	7	25	80	200	554	[69]
Phytic acid-MXene	MB	3–11	25	12	250	42	[70]
MXene@Fe_3O_4	MB	3–11	25	1–40	500	12	[63]

research reported that the –F group has a better affinity for cationic dyes since the electronegativity of F is more significant than that of –O (χF = 3.98, χO = 3.44) [34]. Hence, $Ti_3C_2F_x$ has a better adsorption capacity for MB in theory. When the –F groups are replaced by the –OH group, the H^+ from the acidic environment will compete with the MB^+ ions for $[–O]^–$ adsorption sites and reduce the adsorption efficiency.

The preparation of MXene@Fe_3O_4 through *in-situ* growth progress was developed by Zhang et al. [63]. The adsorption test for MB also has been carried out. The maximum adsorption capacity was up to 11.68 mg/g as the pH of the aqueous solution at 3 or 11. A positive and high value of $\Delta H°$ (>40 kJ/mol) indicated an endothermic adsorption process and intense coordination exchange between MXene@Fe_3O_4 and MB [61,63]. The positive value of $\Delta S°$ and $\Delta G°$ reflected that the adsorption is entropy-driven and energy-driven. Therefore, the increasing temperature may be a benefit for MB removal by adsorption. The date of MB removal on MXene@Fe_3O_4 at 25°C fitted well with the Langmuir model and the increasing adsorptive strength (KL) as the temperature increased, which demonstrated that external energy promoted the interaction. The Dubinin–Radushkevich model showed a mean free energy of less than 8 kJ/mol; it also suggested that physisorption dominated the MB removal process [72]. In a similar study, magnetic $Ti_3C_2T_x$ MXene prepared by the same process hindered the adsorption of cationic dyes such as MB, as the pH of the aqueous solution was lower than 7 [73]. It could be explained that the primary mechanism of adsorption under acidic conditions depended on the formation of hydrogen bonds (Ti–OH…NH) between MB and MXene@Fe_3O_4 instead of the electrostatic interaction.

MXene/polypyrrole (PPy) hybrid was developed and applied for MB removal [69]. Polypyrrole nanoparticles play a role in preventing the MXene from oxidation by changing the surface structure with a wrapping strategy. After two months of storage, MXene/PPy exhibited higher adsorption ability (388 mg/L) than pristine (345 mg/L) for MB. Moreover, the addition of polypyrrole nanoparticles promoted the further stratification of MXene and got larger interlayer spacing. XRD spectrum proved this point: a shift took place in the diffraction peak of (0 0 2) crystal plane from 7.58° to 5.68° after *in-situ* polymerization of PPy nanoparticles, and the crystal plane distance was also changed from 1.17 to 1.56 nm. As a result, an excellent adsorption capacity for MB reached up to 553.57 mg/g. The adsorption kinetics test result is consistent with the pseudo-second-order adsorption model; it indicated that the removal process is dominated by chemical adsorption [74]. The value of $\Delta H°$ ($\Delta H°$ > 60 kJ/mol) also denoted chemical forces as primary interaction in the adsorption process, and this process is endothermic.

3.3. Radionuclide elimination

The characteristics of radionuclides include long half-period, carcinogenicity, and bio-accumulation, which are harmful to the human body. Adsorption is a simple and convenient way to remove radionuclides from polluted wastewater effectively. Some surface functional group formed in the preparation process makes MXene negative charged in general; MXene can electrostatically interact with positively charged nuclides. The mechanism included electrostatic interaction, ion-exchange, inner-sphere complexation, π–π interaction, and hydrogen bonding; it depends on preparation and modification, which may form different structures. These MXene-based adsorbents have been investigated for removing radionuclides from wastewater, as shown in Table 3.

Two recent studies proved the effects of morphological structure and group composition of MXene-based absorbents on removing radioactive iodine. A composite called MXene-PDA-Bi_6O_7 achieved the adsorption equilibrium within 90 min with a maximum adsorption capacity of 64.65 mg/g [80]. Another hybrid called MXene-PIL got a higher maximum uptake capacity of 170 mg/g within 10 min [76]. The adsorption kinetics test showed a higher fitting degree with the pseudo-second-order model, which indicated chemical process dominated the adsorption more than the physical process. The difference in the isothermal model (Freundlich model for MXene-PDA-Bi_6O_7,

Table 3
Comparison of radionuclide adsorption by various MXene-based materials

Material	Pollutant	pH	Temperature (°C)	Pollutant concentration (mg/L)	Materials dose (mg/L)	Maximum uptake (mg/g)	References
Ca^{2+} induced 3D porous MXene gel	U(VI)	5	Room temperature (RT)	100	200	824	[75]
MXene-PIL	Iodide ions	/	RT	254	200	170	[76]
$Ti_3C_2T_x$	Cs^+	6	RT	5	1,000	25	[77]
Ti_2CT_x	U(VI)	3	RT	40	400	213	[78]
nZVI/Alk-$Ti_3C_2T_x$	U(VI)	3.5	RT	100	80	1,315	[79]
TCCH	U(VI)	5	25	200	200	345	[19]
TCCH	Eu(III)	5	25	200	200	97	[19]
MXene-PDA-Bi_6O_7	Iodide ions	5	RT	20	200	65	[80]
Ti_2CT_x	U(VI)	3	25	33.7	100	470	[81]
V_2CT_x	U(VI)	4.5	RT	100	400	174	[82]

Langmuir model for MXene-PIL) may be related to morphological structure. The flower-like MXene-PDA-Bi_6O_7 has fewer exposed sites and prevents adsorbate diffusion from interior sites. Therefore, it is multi-molecular layer adsorption. The low rate constant of the intraparticle diffusion model (0.80399 mg/g·$min^{0.5}$) and high boundary layer thickness of adsorption proved this point [80]. With the layer structure and even-distributed polyimidazole surface group, the MXene-PIL adsorption data is more consistent with the Langmuir model means a relatively uniform single-atom layer adsorption [76].

Wang et al. [81] reported the effect of the number of atomic layers of MXene on U(VI) adsorption. X-ray spectra of uranium form change after sorption showed the reduction of U(VI) to U(IV) on Ti_2CT_x over a pH range of at least 3.0–8.0, while typical nonreductive sorption of U(VI) took place on $Ti_3C_2T_x$. The different reductive abilities of $Ti_3C_2T_x$ and Ti_2CT_x can be rationalized by their different atomic layer structures: the fewer atomic layer, the more reductive abilities the MXene will be, and it will be more advantageous for removing nuclide [16].

The effect of the operating condition, such as pH and temperature, have a consistent tendency (Fig. 4b and c). For a variety of radionuclides such as Th(IV), U(VI) and Eu(III), pH = 5 is a universal optimal adsorption pH [38,78]. At low pH (approximately pH = 2), the H^+ compete with positively charged radionuclides and makes the MXene surface protonated [19]. It minimizes the electrostatic interactions and even leads to a shallow adsorption capacity, as MXene are not negatively charged. Conversely, under high pH (pH > 6), MXene remains negatively charged and can efficiently capture radionuclides [75,82]. This trend also works with other cationic contaminants. After introducing carboxyl, MXene has a lower zeta potential at the same pH [19,38]; it makes MXene negatively charged over a wider pH range and leads to a 99% removal rate of both U(VI) and Eu(III) within short 3 min [19]. Generally, the effect of temperature on radionuclide removal is demonstrated by the adsorption thermodynamics test. There are also similar trends: the positive reaction entropy and enthalpy variations and the negative Gibbs free energy demonstrate that MXene's adsorption of most radionuclides is spontaneous and endothermic.

In summary, the regular open structure and more exposed sites facilitate the adsorption process based on ion-exchange and complexation mechanisms. The admission of a particular group, such as –COOH, may alter its surface charge, thereby making MXene negatively charged over a wide pH range to enhance the adsorption effect of positively charged radionuclides.

4. Modification

The adsorption performance of MXene is significantly related to its surface groups [37], interlayer spacing [68], and surface charge [83]. In addition, drawbacks such as poor antioxidant capacity and dispersibility in non-polar solvents also limit its further application. There are three main modification strategies for the above problems: enlarging the interlayer spacing, introducing the surface group, and improving stability.

4.1. Enlarging the interlayer spacing

A significant challenge in removing ions by MXene is the narrow interlayer space (less than 2 Å), which hinders pollutants with large hydrated ion radii [38]. Delamination of multilayered MXene into few-layered and even superthin nanoflakes may immensely increase the number of active surface sites. However, the stability of the MXene will diminish in an oxygen-rich environment, which manifests itself in a correspondingly exacerbated oxidation and agglomeration [84]. A strategy to overcome this problem is intercalation, which expands the c lattice parameter of MXene to obtain a relatively open structure and more exposed active sites. Cations and small organic molecules are ideal intercalants. Ji et al. [85] investigated the effect of 3-aminopropyltriethoxysilane (APTES) on the structural stability and interlayer space of MXene. After APTES functionalization, APTES and MXene were strongly connected by covalent bonds. Hence, the stability of MXene could be enhanced by preventing contact between MXene and water or dissolved oxygen. Compared with pristine MXene, the interlayer distance of APTES-MXene increased from 24.47 to 35.95 Å; the increment is 11.48 Å. Furthermore, the surface area for APTES-MXene material was 162.67 m^2/g, four times higher than the pristine MXene material. Dimethyl sulfoxide (DMSO) and NaOH play a similar role in extending interlayer space. DMSO can expand the layer spacing of the hydrated MXene by 12.66 Å (from 7.52 to 20.18 Å). These changes lead to more than five times improvement in uptake capacity toward U(VI) [38]. NaOH and KOH intercalations increased the layer spacing of MXene by 4.76 and 6.45 Å, respectively [41,56]. The numerical difference may be caused by differences in the cationic hydration radius, the interlayer space for Alk-$Ti_3C_2T_x$ decrease with increasing metal ionic radius [68]. Although cationic lye is not as effective as small molecule organics in expanding the spacing of layers, alkalization treatment can also introduce a certain amount of –OH, which has considerable advantages in secondary modification and direct utilization [56,68].

4.2. Modification of surface groups

The adjustability of surface groups is a significant advantage of MXene; as the binding site of the contaminant, the number of surface groups determines the adsorption effect. According to previous research, various polar groups such as amines (–NH_2), hydroxyls (–OH), and carboxyl (–COOH) are beneficial for combining with pollutants and facilitating their dispersion in water [86,87]. As mentioned in Section 4.1 – Enlarging the interlayer spacing, more hydroxyl groups exist on the surface of $Ti_3C_2T_x$ nanosheets after alkalinization [42]. After alkalization treatment, it was found that with the decrease of –F groups and the increase of –OH groups, the ion-exchange between MXene and Pb^{2+} was significantly enhanced [44].

The sulfonic groups could be introduced on the surface of MXene through the diazo click reaction, and the introduction of sulfonic acid groups makes the maximum adsorption capacity of Ti_3C_2–SO_3H to MB more than four times that of raw materials [67]. Similarly, the spontaneous grafting of diazo salts by carboxyl sealing on the MXene

surface increases the functional groups by 51.2%, enhancing the adsorption capacity of radionuclides [19]. L-Dopa, silane coupling agents such as APTES and KH570, are also used to introduce groups such as $–NH_2$, –COOH [42,51]. In addition to increasing the functional groups, these reagents also protect MXene from oxidation. This will be discussed in the following subsection. The introduction of functional groups requires consideration of the steric resistance effect [87]. Alkalization pretreatment can alleviate this problem [42], or using polymer monomers as modifiers can also be effectively solved [88].

4.3. Improving the stability

The pristine MXene colloidal solution is susceptible to oxidation after prolonged exposure to water, high temperatures, or ultraviolet (sun) radiation in the air [84]. The Ti atoms at the edge of the MXene sheet are easily oxidized by oxygen atoms, which makes partial adsorption sites lose and decreases the adsorption performance [89]. Nanoparticle wrapping and polymer film-forming strategies can effectively alleviate MXene oxidation to improve the reuse of adsorbents. For instance, positively charged polypyrrole nanoparticles via electrostatic attraction are uniformly deposited on MXene nanosheets, forming a thin film-like substance that protects the edges from oxidation [69]. Silane modification enhances MXene stability by providing a chain structure that blocks oxygen. Compared to the original MXene, the structure of APTES-modified samples can be maintained for up to one month in the presence of water molecules and oxygen molecules, and the long-term stability increases with the increasing APTES concentrations [42,85]. This strategy was also applicable to other silane coupling agents. Typically, hydrophobic silane coupling agents will further improve stability, which is attributed to the formation of hydrophobic surfaces. Different from most modification strategies relying on the surface properties and functional groups of substrates, mussel-inspired chemistry relies on the self-polymerization of dopamine to form PDA films on the surface of materials. PDA films contain high-molecular-weight polymer chains with covalently connected subunits, which also endow materials with antioxidant capacity and a platform for further surface modification [80].

5. Summary and outlook

This review introduced the synthesis of MXene used in adsorption and highlighted the structure of MXene and those strategies that can elevate sorption capacity via changing the structure of MXene. Here, based on the above, the following conclusions are summarized.

- As for preparation strategy, *in-situ* HF etching is suitable for preparing MXene-based adsorbents. In this way, absorbents are endowed with abundant hydrophilic groups and more sites such as –OH, which could combine with various pollutants.
- Relatively open structure, a large layer spacing is conducive to adsorption. However, in a completely open structure, there are inevitable oxidation and agglomeration problems, which are also not conducive to adsorption.
- The introduction of protonizable groups can increase adsorption capacity; in addition, hydrophilic groups can also improve dispersibility, and hydrophobic groups improve stability.
- In terms of modification strategies, the wrapping strategy is applied to restrain oxidation and improve the stability of MXene. The intercalation strategy solves the problem of inter-layer stacking. Meanwhile, both inorganic ions and organic molecules increase the adsorption sites, which is essential for removing contaminants.

MXene is a new generation of layered materials, and the potential for adsorption is undoubtable. Nonetheless, there are still many problems that need to be solved before practical application. The following aspects are important to be addressed in future research:

- It is fundamental to develop new synthetic strategies that introduce a special surface group on MXene while achieving large-scale production in less preparation time.
- It is necessary to develop more thermal stability-improving measures which inhibit oxidation in the edge of MXene.
- It is key to target introducing some surface groups of MXene to eliminate hetero groups inevitably introduced during preparation. So that pollutants are removed more selectively.

Further research, MXene is expected to be an excellent adsorbent to deal with more challenging in water clean.

Declaration of interest

There are no conflicts of interest to declare.

Acknowledgement

This work was supported by Sichuan Youth Science and technology innovation research team (grant number No. 2020JDTD0018) and the Science and Technology Plan Project of Sichuan Province (grant number 2021YFQ0046).

References

[1] N. Khatri, S. Tyagi, Influences of natural and anthropogenic factors on surface and groundwater quality in rural and urban areas, Front. Life Sci., 8 (2015) 23–39.
[2] I. Ali, The quest for active carbon adsorbent substitutes: inexpensive adsorbents for toxic metal ions removal from wastewater, Sep. Purif. Rev., 39 (2010) 95–171.
[3] A. Saravanan, P.S. Kumar, R.V. Hemavathy, S. Jeevanantham, P. Harikumar, G. Priyanka, D.R.A. Devakirubai, A comprehensive review on sources, analysis and toxicity of environmental pollutants and its removal methods from water environment, Sci. Total Environ., 812 (2022) 152456, doi: 10.1016/j.scitotenv.2021.152456.
[4] N. Khandelwal G.K. Darbha, A decade of exploring MXenes as aquatic cleaners: covering a broad range of contaminants, current challenges and future trends, Chemosphere, 279 (2021) 130587, doi: 10.1016/j.chemosphere.2021.130587.

[5] J. Kim, S. Yoon, M. Choi, K.J. Min, K.Y. Park, K. Chon, S. Bae, Metal ion recovery from electrodialysis-concentrated plating wastewater via pilot-scale sequential electrowinning/chemical precipitation, J. Cleaner Prod., 330 (2022) 129879, doi: 10.1016/j.jclepro.2021.129879.
[6] Y. Zhao, S. Kang, L. Qin, W. Wang, T. Zhang, S. Song, S. Komarneni, Self-assembled gels of Fe-chitosan/montmorillonite nanosheets: dye degradation by the synergistic effect of adsorption and photo-Fenton reaction, Chem. Eng. J., 379 (2020) 122322, doi: 10.1016/j.cej.2019.122322.
[7] C. Lu, J. Yang, A. Khan, J. Yang, Q. Li, G. Wang, A highly efficient technique to simultaneously remove acidic and basic dyes using magnetic ion-exchange microbeads, J. Environ. Manage., 304 (2022) 114173, doi: 10.1016/j.jenvman.2021.114173.
[8] L. Ding, L. Li, Y. Liu, Y. Wu, Z. Lu, J. Deng, Y. Wei, J. Caro, H. Wang, Effective ion sieving with $Ti_3C_2T_x$ MXene membranes for production of drinking water from seawater, Nat. Sustainability, 3 (2020) 296–302.
[9] T.A. Khan, E.A. Khan, Shahjahan, Removal of basic dyes from aqueous solution by adsorption onto binary iron-manganese oxide coated kaolinite: non-linear isotherm and kinetics modeling, Appl. Clay Sci., 107 (2015) 70–77.
[10] S.S. Tahir, N. Rauf, Removal of a cationic dye from aqueous solutions by adsorption onto bentonite clay, Chemosphere, 63 (2006) 1842–1848.
[11] M. Yusuf, M. Kumar, M.A. Khan, M. Sillanpää, H. Arafat, A review on exfoliation, characterization, environmental and energy applications of graphene and graphene-based composites, Adv. Colloid Interface Sci., 273 (2019) 102036, doi: 10.1016/j.cis.2019.102036.
[12] M. Zheng, L. Xu, C. Chen, L. Labiadh, B. Yuan, M. Fu, MOFs and GO-based composites as deliberated materials for the adsorption of various water contaminants, Sep. Purif. Technol., 294 (2022) 121187, doi: 10.1016/j.seppur.2022.121187.
[13] S. Zhang, S. Guo, A. Li, D. Liu, H. Sun, F. Zhao, Low-cost bauxite residue-MoS_2 possessing adsorption and photocatalysis ability for removing organic pollutants in wastewater, Sep. Purif. Technol., 283 (2022) 120144, doi: 10.1016/j.seppur.2021.120144.
[14] Y. Wei, P. Zhang, R.A. Soomro, Q. Zhu, B. Xu, Advances in the synthesis of 2D MXenes, Adv. Mater., 33 (2021) 2103148, doi: 10.1002/adma.202103148.
[15] M. Naguib, M. Kurtoglu, V. Presser, J. Lu, J. Niu, M. Heon, L. Hultman, Y. Gogotsi, M.W. Barsoum, Two-dimensional nanocrystals produced by exfoliation of Ti_3AlC_2, Adv. Mater., 23 (2011) 4248–4253.
[16] M. Naguib, V.N. Mochalin, M.W. Barsoum, Y. Gogotsi, 25th anniversary article: MXenes: a new family of two-dimensional materials, Adv. Mater., 26 (2014) 992–1005.
[17] X. Zhang, X.D. Zhao, D.H. Wu, Y. Jing, Z. Zhou, High and anisotropic carrier mobility in experimentally possible Ti_2CO_2 (MXene) monolayers and nanoribbons, Nanoscale, 7 (2015) 16020–16025.
[18] S. Wang, Y. Liu, Q. Lü, H. Zhuang, Facile preparation of biosurfactant-functionalized Ti_2CT_X MXene nanosheets with an enhanced adsorption performance for Pb(II) ions, J. Mol. Liq., 297 (2020) 111810, doi: 10.1016/j.molliq.2019.111810.
[19] P. Zhang, L. Wang, K. Du, S. Wang, Z. Huang, L. Yuan, Z. Li, H. Wang, L. Zheng, Z. Chai, W. Shi, Effective removal of U(VI) and Eu(III) by carboxyl functionalized MXene nanosheets, J. Hazard. Mater., 396 (2020) 122731, doi: 10.1016/j.jhazmat.2020.122731.
[20] J.A. Kumar, P. Prakash, T. Krithiga, D.J. Amarnath, J. Premkumar, N. Rajamohan, Y. Vasseghian, P. Saravanan, M. Rajasimman, Methods of synthesis, characteristics, and environmental applications of MXene: a comprehensive review, Chemosphere, 286 (2022) 131607, doi: 10.1016/j.chemosphere.2021.131607.
[21] O. Kwon, Y. Choi, J. Kang, J.H. Kim, E. Choi, Y.C. Woo, D.W. Kim, A comprehensive review of MXene-based water-treatment membranes and technologies: recent progress and perspectives, Desalination, 522 (2022) 115448, doi: 10.1016/j.desal.2021.115448.
[22] M. Alhabeb, K. Maleski, B. Anasori, P. Lelyukh, L. Clark, S. Sin, Y. Gogotsi, Guidelines for synthesis and processing of two-dimensional titanium carbide ($Ti_3C_2T_x$ MXene), Chem. Mater., 29 (2017) 7633–7644.
[23] P. Srivastava, A. Mishra, H. Mizuseki, K. Lee, A.K. Singh, Mechanistic insight into the chemical exfoliation and functionalization of Ti_3C_2 MXene, ACS Appl. Mater. Interfaces, 8 (2016) 24256–24264.
[24] F. Dixit, K. Zimmermann, R. Dutta, N.J. Prakash, B. Barbeau, M. Mohseni, B. Kandasubramanian, Application of MXenes for water treatment and energy-efficient desalination: a review, J. Hazard. Mater., 423 (2022) 127050, doi: 10.1016/j.jhazmat.2021.127050.
[25] M. Naguib, O. Mashtalir, J. Carle, V. Presser, J. Lu, L. Hultman, Y. Gogotsi, M.W. Barsoum, Two-dimensional transition metal carbides, ACS Nano, 6 (2012) 1322–1331.
[26] F. Liu, A. Zhou, J. Chen, J. Jia, W. Zhou, L. Wang, Q. Hu, Preparation of Ti_3C_2 and Ti_2C MXenes by fluoride salts etching and methane adsorptive properties, Appl. Surf. Sci., 416 (2017) 781–789.
[27] X. Wang, C. Garnero, G. Rochard, D. Magne, S. Morisset, S. Hurand, P. Chartier, J. Rousseau, T. Cabioc'h, C. Coutanceau, V. Mauchamp, S. Célérier, A new etching environment (FeF_3/HCl) for the synthesis of two-dimensional titanium carbide MXenes: a route towards selective reactivity vs. water, J. Mater. Chem. A, 5 (2017) 22012–22023.
[28] J. Halim, M.R. Lukatskaya, K.M. Cook, J. Lu, C.R. Smith, L. Näslund, S.J. May, L. Hultman, Y. Gogotsi, P. Eklund, M.W. Barsoum, Transparent conductive two-dimensional titanium carbide epitaxial thin films, Chem. Mater., 26 (2014) 2374–2381.
[29] A. Lipatov, M. Alhabeb, M.R. Lukatskaya, A. Boson, Y. Gogotsi, A. Sinitskii, Effect of synthesis on quality, electronic properties and environmental stability of individual monolayer Ti_3C_2 MXene flakes, Adv. Electron. Mater., 2 (2016) 1600255, doi: 10.1002/aelm.201600255.
[30] M. Jeon, B. Jun, S. Kim, M. Jang, C.M. Park, S.A. Snyder, Y. Yoon, A review on MXene-based nanomaterials as adsorbents in aqueous solution, Chemosphere, 261 (2020) 127781, doi: 10.1016/j.chemosphere.2020.127781.
[31] F. Shahzad, M. Alhabeb, C.B. Hatter, B. Anasori, S. Man Hong, C.M. Koo, Y. Gogotsi, Electromagnetic interference shielding with 2D transition metal carbides (MXenes), Science, 353 (2016) 1137–1140.
[32] B. Anasori, M.R. Lukatskaya, Y. Gogotsi, 2D metal carbides and nitrides (MXenes) for energy storage, Nat. Rev. Mater., 2 (2017), doi: 10.1038/natrevmats.2016.98.
[33] M.A. Hope, A.C. Forse, K.J. Griffith, M.R. Lukatskaya, M. Ghidiu, Y. Gogotsi, C.P. Grey, NMR reveals the surface functionalisation of Ti_3C_2 MXene, Phys. Chem. Chem. Phys., 18 (2016) 5099–5102.
[34] N. My Tran, Q. Thanh Hoai Ta, A. Sreedhar, J. Noh, $Ti_3C_2T_x$ MXene playing as a strong methylene blue adsorbent in wastewater, Appl. Surf. Sci., 537 (2021) 148006, doi: 10.1016/j.apsusc.2020.148006.
[35] Y. Zhang, J. Lan, L. Wang, Q. Wu, C. Wang, T. Bo, Z. Chai, W. Shi, Adsorption of uranyl species on hydroxylated titanium carbide nanosheet: a first-principles study, J. Hazard. Mater., 308 (2016) 402–410.
[36] J. Guo, Q. Peng, H. Fu, G. Zou, Q. Zhang, Heavy-metal adsorption behavior of two-dimensional alkalization-intercalated MXene by first-principles calculations, J. Phys. Chem. C, 119 (2015) 20923–20930.
[37] I. Persson, L. Näslund, J. Halim, M.W. Barsoum, V. Darakchieva, J. Palisaitis, J. Rosen, P.O.Å. Persson, On the organization and thermal behavior of functional groups on Ti_3C_2 MXene surfaces in vacuum, 2D Mater., 5 (2017), doi: 10.1088/2053–1583/aa89cd.
[38] L. Wang, W. Tao, L. Yuan, Z. Liu, Q. Huang, Z. Chai, J.K. Gibson, W. Shi, Rational control of the interlayer space inside two-dimensional titanium carbides for highly efficient uranium removal and imprisonment, Chem. Commun., 53 (2017) 12084–12087.
[39] Y. Ying, Y. Liu, X. Wang, Y. Mao, W. Cao, P. Hu, X. Peng, Two-dimensional titanium carbide for efficiently reductive removal

of highly toxic chromium(VI) from water, ACS Appl. Mater. Interfaces, 7 (2015) 1795–1803.
[40] O. Mashtalir, M. Naguib, B. Dyatkin, Y. Gogotsi, M.W. Barsoum, Kinetics of aluminum extraction from Ti_3AlC_2 in hydrofluoric acid, Mater. Chem. Phys., 139 (2013) 147–152.
[41] W. Mu, S. Du, Q. Yu, X. Li, H. Wei, Y. Yang, Improving barium ion adsorption on two-dimensional titanium carbide by surface modification, Dalton Trans., 47 (2018) 8375–8381.
[42] G. Zhang, T. Wang, Z. Xu, M. Liu, C. Shen, Q. Meng, Synthesis of amino-functionalized $Ti_3C_2T_x$ MXene by alkalization-grafting modification for efficient lead adsorption, Chem. Commun., 56 (2020) 11283–11286.
[43] Y. Du, B. Yu, L. Wei, Y. Wang, X. Zhang, S. Ye, Efficient removal of Pb(II) by $Ti_3C_2T_x$ powder modified with a silane coupling agent, J. Mater. Sci., 54 (2019) 13283–13297.
[44] Q. Peng, J. Guo, Q. Zhang, J. Xiang, B. Liu, A. Zhou, R. Liu, Y. Tian, Unique lead adsorption behavior of activated hydroxyl group in two-dimensional titanium carbide, J. Am. Chem. Soc., 136 (2014) 4113–4116.
[45] G. Yang, X. Hu, J. Liang, Q. Huang, J. Dou, J. Tian, F. Deng, M. Liu, X. Zhang, Y. Wei, Surface functionalization of MXene with chitosan through *in-situ* formation of polyimidazoles and its adsorption properties, J. Hazard. Mater., 419 (2021) 126220, doi: 10.1016/j.jhazmat.2021.126220.
[46] Y. Lv, K. Chang, H. Wu, P. Fang, C. Chen, Q. Liao, Highly efficient scavenging of Cr(VI) by two-dimensional titanium carbide nanosheets: kinetics, isotherms and thermodynamics analysis, Water Sci. Technol., 84 (2021) 2446–2456.
[47] A. Shahzad, M. Nawaz, M. Moztahida, K. Tahir, J. Kim, Y. Lim, B. Kim, J. Jang, D.S. Lee, Exfoliation of titanium aluminum carbide (211 MAX Phase) to form nanofibers and two-dimensional nanosheets and their application in aqueous-phase cadmium sequestration, ACS Appl. Mater. Interfaces, 11 (2019) 19156–19166.
[48] A. Shahzad, K. Rasool, W. Miran, M. Nawaz, J. Jang, K.A. Mahmoud, D.S. Lee, Mercuric ion capturing by recoverable titanium carbide magnetic nanocomposite, J. Hazard. Mater., 344 (2018) 811–818.
[49] A. Shahzad, M. Nawaz, M. Moztahida, J. Jang, K. Tahir, J. Kim, Y. Lim, V.S. Vassiliadis, S.H. Woo, D.S. Lee, $Ti_3C_2T_x$ MXene core-shell spheres for ultrahigh removal of mercuric ions, Chem. Eng. J., 368 (2019) 400–408, doi: 10.1016/j.cej.2019.02.160.
[50] X. Hu, C. Chen, D. Zhang, Y. Xue, Kinetics, isotherm and chemical speciation analysis of Hg(II) adsorption over oxygen-containing MXene adsorbent, Chemosphere, 278 (2021) 130206, doi: 10.1016/j.chemosphere.2021.130206.
[51] D. Gan, Q. Huang, J. Dou, H. Huang, J. Chen, M. Liu, Y. Wen, Z. Yang, X. Zhang, Y. Wei, Bioinspired functionalization of MXenes ($Ti_3C_2T_X$) with amino acids for efficient removal of heavy metal ions, Appl. Surf. Sci., 504 (2020) 144603, doi: 10.1016/j.apsusc.2019.144603.
[52] A. Shahzad, K. Rasool, W. Miran, M. Nawaz, J. Jang, K.A. Mahmoud, D.S. Lee, Two-dimensional $Ti_3C_2T_x$ MXene nanosheets for efficient copper removal from water, ACS Sustainable Chem. Eng., 5 (2017) 11481–11488.
[53] X. Feng, Z. Yu, R. Long, X. Li, L. Shao, H. Zeng, G. Zeng, Y. Zuo, Self-assembling 2D/2D (MXene/LDH) materials achieve ultra-high adsorption of heavy metals Ni^{2+} through terminal group modification, Sep. Purif. Technol., 253 (2020) 117525, doi: 10.1016/j.seppur.2020.117525.
[54] A.K. Fard, G. Mckay, R. Chamoun, T. Rhadfi, H. Preud'Homme, M.A. Atieh, Barium removal from synthetic natural and produced water using MXene as two dimensional (2-D) nanosheet adsorbent, Chem. Eng. J., 317 (2017) 331–342.
[55] C.E. Ren, K.B. Hatzell, M. Alhabeb, Z. Ling, K.A. Mahmoud, Y. Gogotsi, Charge- and size-selective ion sieving through $Ti_3C_2T_x$ MXene membranes, J. Phys. Chem. Lett., 6 (2015) 4026–4031.
[56] X. Zhu, B. Liu, H. Hou, Z. Huang, K.M. Zeinu, L. Huang, X. Yuan, D. Guo, J. Hu, J. Yang, Alkaline intercalation of Ti_3C_2 MXene for simultaneous electrochemical detection of Cd(II), Pb(II), Cu(II) and Hg(II), Electrochim. Acta, 248 (2017) 46–57.
[57] W. Yang M. Cao, Study on the difference in adsorption performance of graphene oxide and carboxylated graphene oxide for Cu(II), Pb(II) respectively and mechanism analysis, Diamond Relat. Mater., 129 (2022) 109332, doi: 10.1016/j.diamond.2022.109332.
[58] B. Jun, N. Her, C.M. Park, Y. Yoon, Effective removal of Pb(II) from synthetic wastewater using $Ti_3C_2T_x$ MXene, Environ. Sci. Water Res. Technol., 6 (2020) 173–180.
[59] V.V. Dev, K.K. Nair, G. Baburaj, K.A. Krishnan, Pushing the boundaries of heavy metal adsorption: a commentary on strategies to improve adsorption efficiency and modulate process mechanisms, Colloid Interface Sci. Commun., 49 (2022) 100626, doi: 10.1016/j.colcom.2022.100626.
[60] Y. Feng, H. Wang, J. Xu, X. Du, X. Cheng, Z. Du, H. Wang, Fabrication of MXene/PEI functionalized sodium alginate aerogel and its excellent adsorption behavior for Cr(VI) and Congo red from aqueous solution, J. Hazard. Mater., 416 (2021) 125777, doi: 10.1016/j.jhazmat.2021.125777.
[61] G.B. Oguntimein, Biosorption of dye from textile wastewater effluent onto alkali treated dried sunflower seed hull and design of a batch adsorber, J. Environ. Chem. Eng., 3 (2015) 2647–2661.
[62] B. Jun, J. Heo, N. Taheri-Qazvini, C.M. Park, Y. Yoon, Adsorption of selected dyes on $Ti_3C_2T_x$ MXene and Al-based metal-organic framework, Ceram. Int., 46 (2020) 2960–2968.
[63] P. Zhang, M. Xiang, H. Liu, C. Yang, S. Deng, Novel two-dimensional magnetic titanium carbide for methylene blue removal over a wide pH range: insight into removal performance and mechanism, ACS Appl. Mater. Interfaces, 11 (2019) 24027–24036.
[64] B. Sun, X. Dong, H. Li, Y. Shang, Y. Zhang, F. Hu, S. Gu, Y. Wu, T. Gao, G. Zhou, Surface charge engineering for two-dimensional Ti_2CT_x MXene for highly efficient and selective removal of cationic dye from aqueous solution, Sep. Purif. Technol., 272 (2021) 118964, doi: 10.1016/j.seppur.2021.118964.
[65] Z. Zhang, J. Xu, X. Yang, MXene/sodium alginate gel beads for adsorption of methylene blue, Mater. Chem. Phys., 260 (2021) 124123, doi: 10.1016/j.matchemphys.2020.124123.
[66] H. Lei, Z. Hao, K. Chen, Y. Chen, J. Zhang, Z. Hu, Y. Song, P. Rao, Q. Huang, Insight into adsorption performance and mechanism on efficient removal of methylene blue by accordion-like V_2CT_x MXene, J. Phys. Chem. Lett., 11 (2020) 4253–4260.
[67] Y. Lei, Y. Cui, Q. Huang, J. Dou, D. Gan, F. Deng, M. Liu, X. Li, X. Zhang, Y. Wei, Facile preparation of sulfonic groups functionalized MXenes for efficient removal of methylene blue, Ceram. Int., 45 (2019) 17653–17661.
[68] Z. Wei, Z. Peigen, T. Wubian, Q. Xia, Z. Yamei, S. Zheng Ming, Alkali treated $Ti_3C_2T_x$ MXenes and their dye adsorption performance, Mater. Chem. Phys., 206 (2018) 270–276.
[69] X. Shi, M. Gao, W. Hu, D. Luo, S. Hu, T. Huang, N. Zhang, Y. Wang, Largely enhanced adsorption performance and stability of MXene through *in-situ* depositing polypyrrole nanoparticles, Sep. Purif. Technol., 287 (2022) 120596, doi: 10.1016/j.seppur.2022.120596.
[70] C. Cai, R. Wang, S. Liu, X. Yan, L. Zhang, M. Wang, Q. Tong, T. Jiao, Synthesis of self-assembled phytic acid-MXene nanocomposites via a facile hydrothermal approach with elevated dye adsorption capacities, Colloids Surf., A, 589 (2020) 124468, doi: 10.1016/j.colsurfa.2020.124468.
[71] O. Mashtalir, K.M. Cook, V.N. Mochalin, M. Crowe, M.W. Barsoum, Y. Gogotsi, S.A.T.C. Energy Frontier Research Centers EFRC United States Fluid Interface Reactions, Dye adsorption and decomposition on two-dimensional titanium carbide in aqueous media, J. Mater. Chem. A, 2 (2014) 14334–14338.
[72] Z. Zhu, M. Xiang, L. Shan, T. He, P. Zhang, Effect of temperature on methylene blue removal with novel 2D-Magnetism titanium carbide, J. Solid State Chem., 280 (2019) 120989, doi: 10.1016/j.jssc.2019.120989.
[73] M. Rethinasabapathy, G. Bhaskaran, B. Park, J. Shin, W. Kim, J. Ryu, Y.S. Huh, Iron oxide (Fe_3O_4)-laden titanium carbide ($Ti_3C_2T_x$) MXene stacks for the efficient sequestration of cationic

dyes from aqueous solution, Chemosphere, 286 (2022) 131679, doi: 10.1016/j.chemosphere.2021.131679.
[74] Y.S. Ho G. McKay, Pseudo-second-order model for sorption processes, Process Biochem., 34 (1999) 451–465.
[75] Z. He, D. Huang, G. Yue, J. Zhu, P. Zhao, Ca^{2+} induced 3D porous MXene gel for continuous removal of phosphate and uranium, Appl. Surf. Sci., 570 (2021) 150804, doi: 10.1016/j.apsusc.2021.150804.
[76] S. Sun, X. Sha, J. Liang, G. Yang, X. Hu, Z. He, M. Liu, N. Zhou, X. Zhang, Y. Wei, Rapid synthesis of polyimidazole functionalized MXene via microwave-irradiation assisted multi-component reaction and its iodine adsorption performance, J. Hazard. Mater., 420 (2021) 126580, doi: 10.1016/j.jhazmat.2021.126580.
[77] A.R. Khan, S.M. Husnain, F. Shahzad, S. Mujtaba-Ul-Hassan, M. Mehmood, J. Ahmad, M.T. Mehran, S. Rahman, Two-dimensional transition metal carbide ($Ti_3C_2T_x$) as an efficient adsorbent to remove cesium (Cs(+)), Dalton Trans., 48 (2019) 11803–11812.
[78] S. Li, L. Wang, J. Peng, M. Zhai, W. Shi, Efficient thorium(IV) removal by two-dimensional Ti_2CT_x MXene from aqueous solution, Chem. Eng. J., 366 (2019) 192–199.
[79] S. Wang, L. Wang, Z. Li, P. Zhang, K. Du, L. Yuan, S. Ning, Y. Wei, W. Shi, Highly efficient adsorption and immobilization of U(VI) from aqueous solution by alkalized MXene-supported nanoscale zero-valent iron, J. Hazard. Mater., 408 (2021) 124949, doi: 10.1016/j.jhazmat.2020.124949.
[80] X. Sha, H. Huang, S. Sun, H. Huang, Q. Huang, Z. He, M. Liu, N. Zhou, X. Zhang, Y. Wei, Mussel-inspired preparation of MXene-PDA-Bi_6O_7 composites for efficient adsorptive removal of iodide ions, J. Environ. Chem. Eng., 8 (2020) 104261, doi: 10.1016/j.jece.2020.104261.
[81] L. Wang, H. Song, L. Yuan, Z. Li, Y. Zhang, J.K. Gibson, L. Zheng, Z. Chai, W. Shi, Efficient U(VI) reduction and sequestration by Ti_2CT_x MXene, Environ. Sci. Technol., 52 (2018) 10748–10756.
[82] L. Wang, L. Yuan, K. Chen, Y. Zhang, Q. Deng, S. Du, Q. Huang, L. Zheng, J. Zhang, Z. Chai, M.W. Barsoum, X. Wang, W. Shi, Loading actinides in multilayered structures for nuclear waste treatment: the first case study of uranium capture with vanadium carbide MXene, ACS Appl. Mater. Interfaces, 8 (2016) 16396–16403.
[83] H. Riazi, M. Anayee, K. Hantanasirisakul, A.A. Shamsabadi, B. Anasori, Y. Gogotsi, M. Soroush, Surface modification of a MXene by an aminosilane coupling agent, Adv. Mater. Interfaces, 7 (2020) 1902008, doi: 10.1002/admi.201902008.
[84] C.J. Zhang, S. Pinilla, N. McEvoy, C.P. Cullen, B. Anasori, E. Long, S. Park, A. Seral-Ascaso, A. Shmeliov, D. Krishnan, C. Morant, X. Liu, G.S. Duesberg, Y. Gogotsi, V. Nicolosi, Oxidation stability of colloidal two-dimensional titanium carbides (MXenes), Chem. Mater., 29 (2017) 4848–4856.
[85] J. Ji, L. Zhao, Y. Shen, S. Liu, Y. Zhang, Covalent stabilization and functionalization of MXene via silylation reactions with improved surface properties, FlatChem, 17 (2019) 100128, doi: https://doi.org/10.1016/j.flatc.2019.100128.
[86] A.K. Gaharwar, N.A. Peppas, A. Khademhosseini, Nanocomposite hydrogels for biomedical applications, Biotechnol. Bioeng., 111 (2014) 441–453.
[87] Y. Huan, G. Wang, C. Li, G. Li, Acrylic acid grafted-multi-walled carbon nanotubes and their high-efficiency adsorption of methylene blue, J. Mater. Sci., 55 (2020) 4656–4670.
[88] C. Hao, G. Li, G. Wang, W. Chen, S. Wang, Preparation of acrylic acid modified alkalized MXene adsorbent and study on its dye adsorption performance, Colloids Surf., A, 632 (2022) 127730, doi: 10.1016/j.colsurfa.2021.127730.
[89] Y. Dall'Agnese, M.R. Lukatskaya, K.M. Cook, P. Taberna, Y. Gogotsi, P. Simon, High capacitance of surface-modified 2D titanium carbide in acidic electrolyte, Electrochem. Commun., 48 (2014) 118–122.